

Analyses of Humanoid Visual Lifting Biped-walking and Spontaneous Arms' Swinging by Dynamical Coupling

Jumpei Nishiguchi¹, Tomohide Maeba¹, Gyetak Lee¹, Mamoru Minami¹ and Akira Yanou¹

¹ Graduate School of Natural Science and Technology, Okayama University Tsushimanaka 3-1-1, Okayama, JAPAN.
(Tel: 81-86-251-8924)

¹nishiguchi@suri.sys.okayama-u.ac.jp

Abstract: Biped locomotion created by a controller based on Zero-Moment Point [ZMP] known as reliable control method looks different from human's walking on the view point that ZMP-based walking does not include falling state. However, the walking control that does not depend on ZMP is vulnerable to turnover. Therefore, keeping the walking of dynamical motion stable is inevitable issue for realization of human-like natural walking—we call the humans' walking that includes toe off states as "natural." In this paper, walking model including slipping, bumping, surface-contacting and point-contacting of foot is discussed. Then, we propose a "Visual-Lifting Control" method to enhance standing robustness and prevent the robot from falling down without utilizing ZMP, i.e., whose walking involve falling down states. Simulation results indicate that this strategy helps stabilize bipedal walking even though ZMP is not kept inside convex hull of supporting area. Moreover, we point out that arms begin to swing spontaneously by dynamical coupling among body links without input torques concerning the arms' joints.

Keywords: Visual servo, Strongly Stable, Arms' swing

1 INTRODUCTION

As for walking control of the humanoid, ZMP-based walking is known as the most potential approach, which has been proved to be a realistic control strategy to demonstrate stable walking of actual biped robots, since it can guarantee that the robots can keep standing by retaining the ZMP within the convex hull of supporting area [1], [2]. Instead of the ZMP, another approaches that put the importance on keeping the robot's walking trajectories inside of a basin of attraction [3]-[5] including a method referring limit cycle to determine input torque [6].

These previous discussions are based on simplified bipedal models, which tend to avoid discussing the effects of feet or slipping existing in real world. Contrarily to the above references, a research [7] has pointed out that the effect of foot bears varieties of the walking gait, e.g., point contacting (heel contacting) and surface contacting (foot sole contacting with ground), causing changing of dimension of state variables. Our research has begun from such view point of [7] as aiming at describing gait's dynamics as correctly as possible, including point/surface-contacting state of foot, slipping of the foot and bumping, where walking gait states transfer based on the past walking motions, called event-driven. However, our model differs from [7] in that it uses leg model without body, arms and head, instead of that we discuss the dynamics of whole-body humanoid. And that what the authors think important is that the dimension of dynamical equation will change depending on the walking gaits' varieties, which introduced by [8] concerning one-legged hopping robot.

Given as an example that heel be detached from ground while its toe being contacting, a new state variable describing foot's rotation would emerge, resulting in an increase of a number of state variables. In fact, this kind of dynamics with the dimension number of state variables being changed by the result of its dynamical time profiles of motions are out of the arena of control theory that discusses how to control a system with fixed states' number. Further the tipping over motion has been called as non-holonomic dynamics that includes a joint without inputting torque, i.e., free joint.

Meanwhile, landing of the heel or the toe of lifting leg in the air to the ground makes a geometrical contact. [9] mentioned how to represent contacting with environment that can handle constraint motion with friction by algebraic equation and applied it to human figures [10]. On the basis of these references, we derive dynamics of eleven kinds of gaits including slipping motion with both varying constraint conditions and changing of the dimension of state variables where the humanoid's dynamical model has been elaborated as much as possible.

When ZMP is to be on the edge of convex hull of foot, meaning the humanoid is in a state of toe-off, the gait deems to be unstable. In this paper, ZMP-independent walking is proposed to realize human-like natural walking including toe-off state, that is a method to enhance standing robustness named "Visual-Lifting Control" based on visual servoing and visual feedback concept, which is based on a similar concept of impedance control method [16]. We utilize real-time pose tracking method to observe a static object that is set in front of the robot to measure the robot's head position/orientation

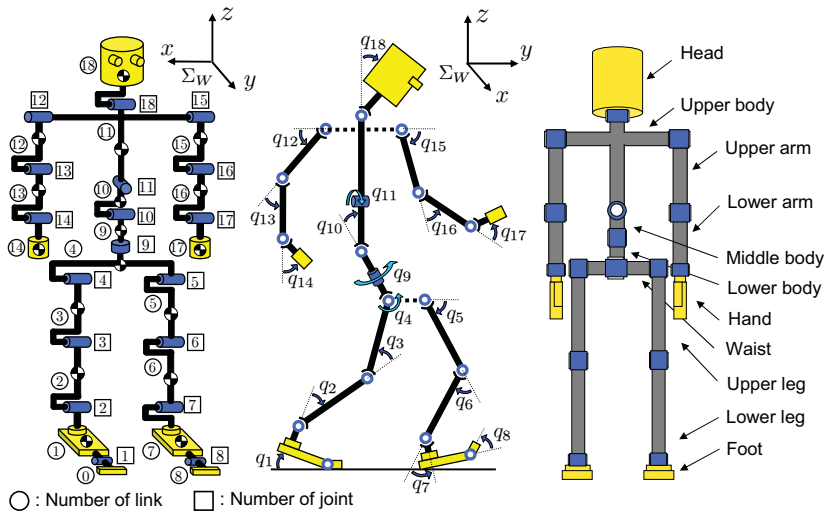


Fig. 1. Definition of humanoid's link, joint and angle number

based on the object through visual pose estimation [17], [18] during walking. The simulation results show that visual feedback helps realize stable bipedal walking that ZMP is not kept within convex hull of supporting area on condition that humanoid's dynamics includes toe-off, slipping and bumping. Moreover, through the motion of arms and body, we verifies that both arms begin to swing spontaneously and asymmetrically by internal dynamical coupling among body links even though input torques for both arms are set to be always zero.

2 DYNAMICAL WALKING MODEL

We discuss a biped robot whose definition is depicted in Fig. 1. Table 1 indicates length l_i [m], mass m_i [kg] of links and joints' coefficient of viscous friction d_i [N·m·s/rad], which are decided based on [11]. Our model represents rigid whole body—feet including toe, torso, arms and body—having 18 degree-of-freedom. Detail explanation of this model is omitted, which is described in [19].

3 WALKING GAIT TRANSITION

Figure 2 also depicts possible gait transition of bipedal walking based on event-driven, which indicate that appropriate dynamics and variables are selected and applied according to the state. In the state that has ramification such as state (III) in Fig. 2 into state (III') or (IV) or (V), the gait is switched to next state in case that auxiliary switching condition written above the allow in the figure indicating phase transient is satisfied. In the gait transition from (V') or (VI') to (VII), supporting-foot is switched from one foot to the other foot with renumbering of link, joint and angle's number. What the authors want to emphasize here is that the varieties of this transition completely depend on the so-

Table 1. Physical parameters

Link	l_i	m_i	d_i
Head	0.24	4.5	0.5
Upper body	0.41	21.5	10.0
Middle body	0.1	2.0	10.0
Lower body	0.1	2.0	10.0
Upper arm	0.31	2.3	0.03
Lower arm	0.24	1.4	1.0
Hand	0.18	0.4	2.0
Waist	0.27	2.0	10.0
Upper leg	0.38	7.3	10.0
Lower leg	0.40	3.4	10.0
Foot	0.07	1.1	10.0
Total	1.7	63.8	

lution of dynamics. A condition that heel of supporting-foot detaches from the ground in Fig. 2 (I), (III), (III'), (V) to (II), (IV), (IV'), (VI) was discussed in [19].

When floating-foot attaches to ground, we need to consider heel/toe-strike motion. We assume that this heel/toe-strike can be represented by completely inelastic collision introduced in [7]. Figure 2 has two kinds of bumping concerning heel and toe. We denoted dynamics of bumping between the heel and the ground in [19].

4 VISUAL-LIFTING CONTROL

4.1 Feedback lifting torque generator

This section propose a vision-feedback control for improving humanoid's standing/walking stability as shown in Fig. 3. We use a model-based matching method to measure pose of a static target object denoted by $\psi(t)$ based on Σ_H , which represents the robot's head. The desired relative pose of Σ_R (reference target object's coordinate) and Σ_H is predefined by Homogeneous Transformation as ${}^H T_R$. The difference of the desired head pose Σ_{H_d} and the current pose Σ_H is denoted as ${}^H T_{H_d}$, it can be described by:

$${}^H T_{H_d}(\psi_d(t), \psi(t)) = {}^H T_R(\psi(t)) \cdot {}^{H_d} T_R^{-1}(\psi_d(t)), \quad (1)$$

where, although ${}^H T_R$ is calculated by $\psi(t)$ that can measured by on-line visual pose estimation method [17], [18], we assume this parameter as being detected correctly in this paper. Here, the force exerted on the head to minimize $\delta\psi(t) = \psi_d(t) - \psi(t)$ calculated from ${}^H T_{H_d}$ —the pose deviation of the robot's head caused by gravity force and walking dynamical influences—is considered to be directly proportional to $\delta\psi(t)$. The joint torque $\tau_h(t)$ that pulls the

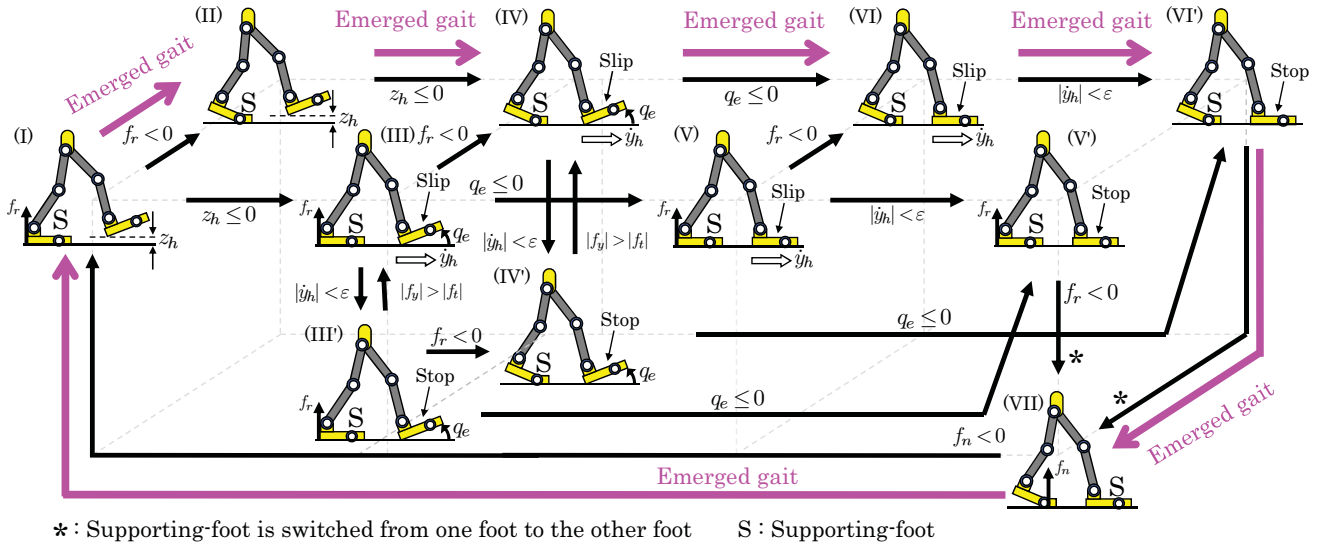


Fig. 2. State, gait's transition and emerged walking gait

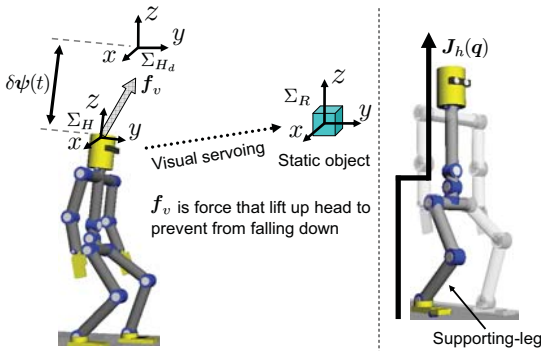


Fig. 3. Concept of Visual-Lifting Control

robot's head up is given the following equation:

$$\tau_h(t) = J_h(q)^T K_p \delta\psi(t), \quad (2)$$

where $J_h(q)$ in Fig. 3 is Jacobian matrix of the head pose against joint angles including $q_1, q_2, q_3, q_4, q_9, q_{10}, q_{11}, q_{18}$, and K_p means proportional gain similar to impedance control. We use this input to compensate the falling motions caused by gravity or dangerous slipping motion happened unpredictably during all walking states in Fig. 2. Notice that the input torque for non-holonomic joint like joint-1 (toe of supporting-foot), τ_{h1} in $\tau_h(t)$ in Eq. (2) is to be set as zero since it is free joint. Although $\delta\psi(t)$ can represent error concerning the humanoid's both position and orientation, only position was utilized in this research, so K_p was set as $K_p = \text{diag}[20, 290, 1100]^T$.

4.2 Feedforward leg and body motion generator

In addition to $\tau_h(t)$, we used two input torques: $\tau_t(t) = [0, \dots, 0, \tau_{t5}, 0, \dots, 0]^T$ to make floating-leg (joint-5) step forward and $\tau_w(t) = [0, \dots, 0, \tau_{w11}, 0, \dots, 0]^T$ to swing waist's roll angle (joint-11) according to supporting-foot.

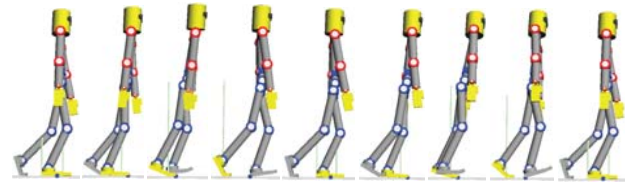


Fig. 4. Screen-shot of bipedal walking

The element τ_{t5} and τ_{w11} of $\tau_t(t)$ and $\tau_w(t)$ are shown below:

$$\tau_{t5} = 20 \cos \{2\pi(t - t_1)/1.85\}, \quad (3)$$

$$\tau_{w11} = \begin{cases} 50 \sin \{2\pi(t - t_1)/1.85\} & (\text{if Right leg}) \\ -50 \sin \{2\pi(t - t_1)/1.85\} & (\text{if Left leg}). \end{cases} \quad (4)$$

Here, t_1 means the time that supporting-foot and contacting-foot are switched described in section IV and V.

4.3 Combined lifting/swinging controller

Combining three torque generators expressed as Eqs. (2), (3) and (4), a controller for walking is created as $\tau(t) = \tau_h(t) + \tau_t(t) + \tau_w(t)$.

5 EXAMPLE OF BIPEDAL WALKING

Under the environment that sampling time was set as 3.0×10^{-3} [sec] and friction force between foot and the ground as $f_t = 0.7f_{n2}$, the following simulations were conducted. In regard to simulation environment, we used "Borland C++ Builder Professional Ver. 5.0" to make simulation program and "OpenGL Ver. 1.5.0" to display humanoid's time-transient configurations.

5.1 Analyses of walking motion

The humanoid walked as shown in Fig. 4 and the followings are the results: average length of stride is 0.43 [m] and walking speed is 2.15 [km/h]. Figures 5, 6 show state

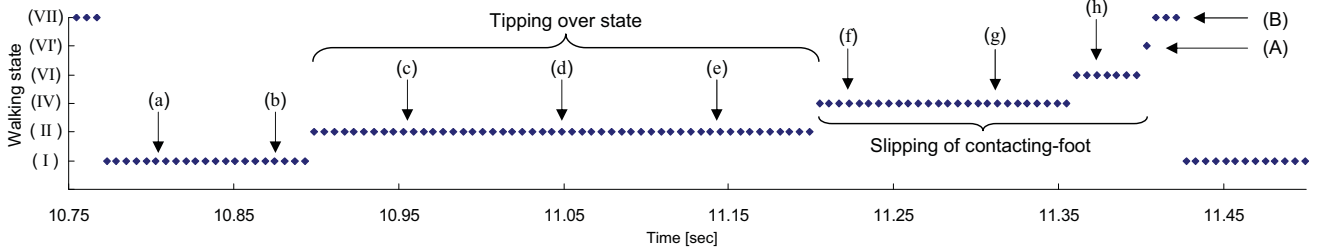


Fig. 5. State transition of walking in one step

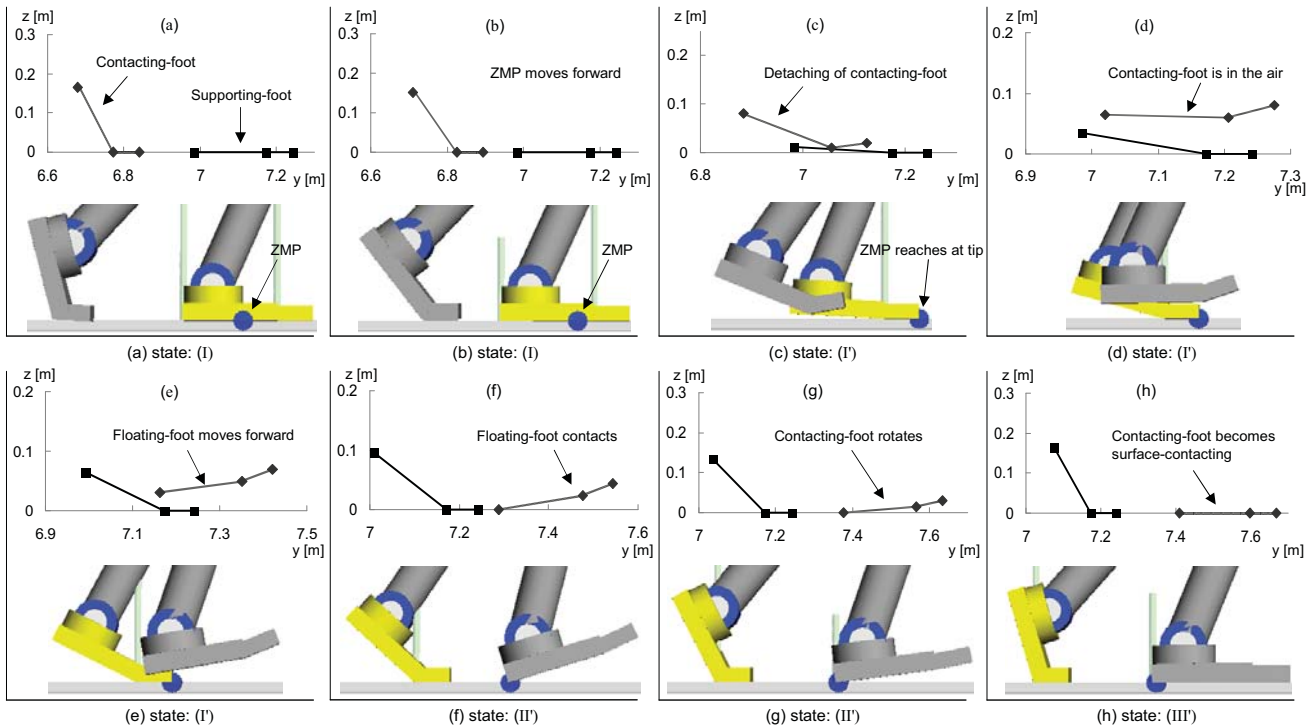


Fig. 6. Feet's position in y - z plain (Σ_W) and displacement of ZMP during one walking step

transition generated by the humanoid's dynamics, both feet's position in y - z plain and displacement of ZMP during one walking step. In this simulation, the humanoid walked in accordance with the following path: (I) \rightarrow (II) \rightarrow (IV) \rightarrow (VI) \rightarrow (VI') \rightarrow (VII) \rightarrow (I) \rightarrow ... in Fig. 2 as "Emerged gait." This transition was selected among all possible transient in Fig. 2 by the closed loop dynamics. Figure 5 depicts walking states transition (I to VII) defined in Fig. 2. against time in horizontal axis, where (a) to (h) represent selected time in the walking motion and (a) to (h) correspond to the feet's contacting states depicted in Fig. 6. As you see in (a) and (b) in Fig. 6, the ZMP is inside foot's contacting sole, and it exists at fringe of tiptoe from (c) to (e), describing states (c) to (e) are in toe-off as written in Fig. 5 "toe-off state." The states from (f) to (h) include slipping of contacting-foot. After the slipping, a state (VI') pointed by "(A)" appears, indicating the both feet are stopping transiently and the state (VI') changed into (VII) pointed by "(B)" describing kicking motion of rear foot and the definition of supporting-foot

and contacting-foot is alternated in this state. In addition, we confirmed contacting-foot's slipping as shown in Fig. 7. Left side means the relation of displacement and velocity of the contacting-foot's heel in walking direction, i.e., y -axis in Fig. 1, and right side is shape of the foot's transient from heel's contacting to surface-contacting in y - z plane. This figure indicates that the foot's slipping velocity decreases and converges to zero and the foot slips about 9 [cm] after toe contacts to the ground.

Figure 8 depicts trajectory of neck (origin of link-18) in 3-D space representation, excluding a trajectory in transient state corresponding to 0–20 steps, this means that the walking motion converged into limit cycle after 21 walking steps. Then, the trajectories that are separated into two plane (x - y plane and y - z plane) from initial condition to 200 steps are shown in Fig. 9. We can confirm that motion concerning left side and right side against the dotted line is symmetric, which means the neck and shoulder swung along with y -axis given at Fig. 9, representing rolling motion of upper body.

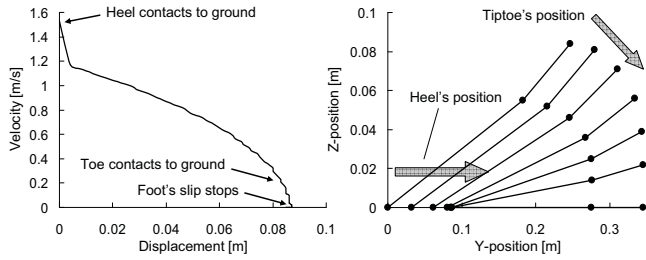


Fig. 7. Slipping motion of contacting-foot

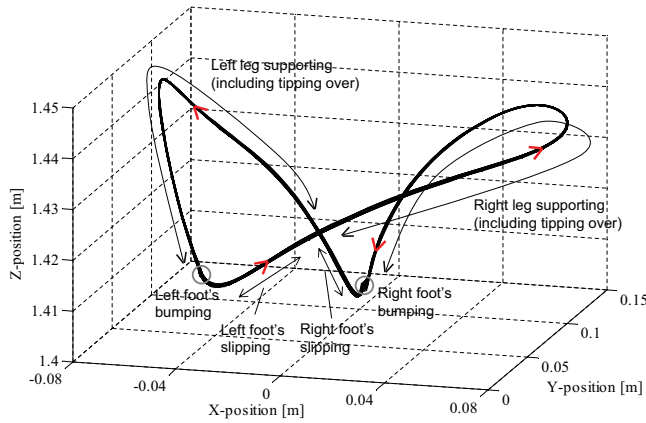


Fig. 8. Emerged limit cycle [(x, y, z) trajectory of neck]

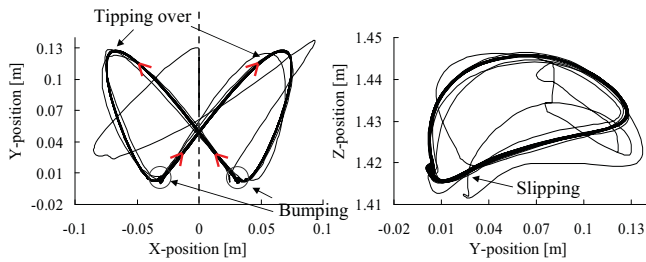


Fig. 9. Motion trajectory of neck

The right graph representing neck's motion in y - z plane, the neck swayed in sagittal plane forward and backward with height varying by walking states including bumping (contacting) state in it. These figures implies that visual feedback has stabilized the walking including gait's transition and motions as shown in Figs. 2, 6, 7 including toe-off, bumping, slipping and change of state variables.

5.2 Spontaneous arms' swinging

Figure 10 shows angles of arms (q_{12} and q_{15}) in Fig. 4. Although we set $q_{12}(0) = q_{15}(0) = 0.2$ [rad] and $\dot{q}_{12}(0) = \dot{q}_{15}(0) = 0.0$ [rad/s] as initial condition and there was no input torques to arms and hands while walking, the arms began to swing spontaneously and asymmetrically. On the other hand, the arms' motion changed like Fig. 11 when input torque expressed as Eq. (4) is not used. Compared with Fig. 10, the arms' amplitude decreased by 72% and both

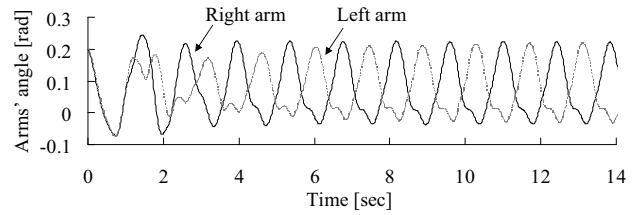


Fig. 10. Arms' swing with $\tau_w(t)$

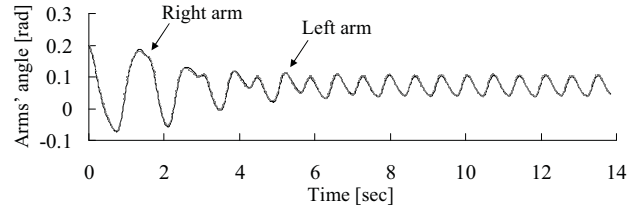


Fig. 11. Arms' swing without $\tau_w(t)$

arms' oscillations are not asymmetric. Therefore, we can say that both arms' swing were caused by internal dynamical coupling among links, especially the motion of body's roll angle affects the arms' swing. In this paper, "dynamical coupling" is defined as torque that is given by non-diagonal element of inertia matrix.

Firstly, dynamical coupling torque $M_{12,11}\ddot{q}_{11}$ from body's roll angle (joint-11) to right arm (joint-12) is shown in Fig. 12. Here, $M_{i,j}$ means i -th row and j -th column in inertia matrix $M(\mathbf{q})$. On the other hand, Fig. 13 means coupling torque $M_{9,11}\ddot{q}_{11}$ from body's roll angle to body's yaw angle (joint-9). These figures imply that input torque expressed as Eq. (4) vibrates yaw angle, meaning motion of roll angle does not transmit directly to the arm as coupling. Then, Fig. 14 shows coupling torque $M_{12,9}\ddot{q}_9$ from body's yaw angle to right arm. This figure indicates that motion of yaw angle that is induced by Eq. (4) generates arm's swing.

6 CONCLUSION

As a first step to realize human-like natural walking, strict dynamical model that contains flat feet including toe, slipping and bumping was created in this paper. Then, we proposed Visual-Lifting Control based on visual feedback as a strategy that prevents turnover generated by unpredictable slipping or unstable gaits.

From simulation results, we confirmed that the proposed strategy could help realize a ZMP-independent walking and converge walking trajectory that is generated by varieties of dynamics and gait to limit cycle. Moreover, we verified arm's motion based on internal dynamical coupling and pointed out that motion of body's roll angle is essential for arm's spontaneous and asymmetric swing even though input torques of both arms were set to be always zero.

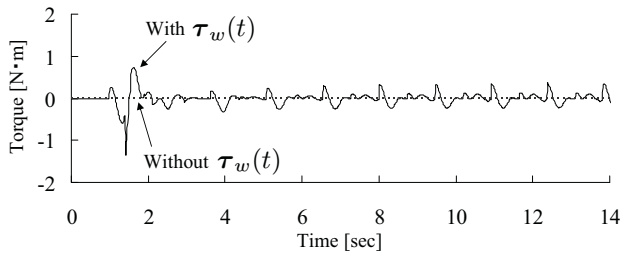


Fig. 12. Dynamical coupling between roll angle and right arm

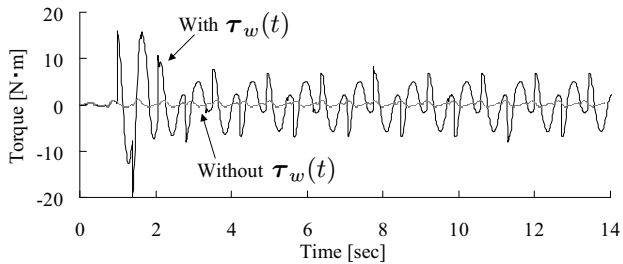


Fig. 13. Dynamical coupling between roll angle and yaw angle

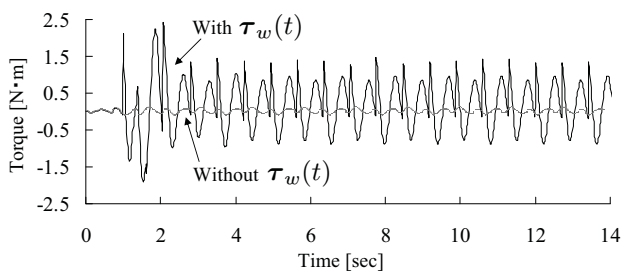


Fig. 14. Dynamical coupling between yaw angle and right arm

REFERENCES

[1] M. Vukobratovic, A. Frank and D. Juricic, "On the Stability of Biped Locomotion," *IEEE Transactions on Biomedical Engineering*, Vol.17, No.1, 1970.

[2] M. Vukobratovic and J. Stepanenko, "On the Stability of Anthropomorphic Systems," *Mathematical Biosciences*, Vol.15, pp.1-37, 1972.

[3] S. Colins, A. Ruina, R. Tedrake and M. Wisse, "Efficient Bipedal Robots Based on Passive-Dynamic Walkers," *Science*, Vol.307, pp.1082-1085, 2005.

[4] J. Pratt, P. Dilworth and G. Pratt, "Virtual Model Control of a Bipedal Walking Robot," *Proceedings of IEEE International Conference on Robotics and Automation*, pp.193-198, 1997.

[5] R.E. Westervelt, W.J. Grizzle and E.D. Koditschek, "Hybrid Zero Dynamics of Planar Biped Walkers," *IEEE Transactions on Automatic Control*, Vol.48, No.1, pp.42-56, 2003.

[6] Y. Harada, J. Takahashi, D. Nenchev and D. Sato, "Limit Cycle Based Walk of a Powered 7DOF 3D Biped with Flat Feet," *Proceedings of IEEE/RSJ International Conference on Intelligent Robots and Systems*, pp.3623-3628, 2010.

[7] Y. Huang, B. Chen, Q. Wang, K. Wei and L. Wang, "Energetic efficiency and stability of dynamic bipedal walking gaits with

different step lengths," *Proceedings of IEEE/RSJ International Conference on Intelligent Robots and Systems*, pp.4077-4082, 2010.

[8] T. Wu, T. Yeh and B. Hsu, "Trajectory Planning of a One-Legged Robot Performing Stable Hop," *Proceedings of IEEE/RSJ International Conference on Intelligent Robots and Systems*, pp.4922-4927, 2010.

[9] Y. Nakamura and K. Yamane, "Dynamics of Kinematic Chains with Discontinuous Changes of Constraints—Application to Human Figures that Move in Contact with the Environments—," *Journal of RSJ*, Vol.18, No.3, pp.435-443, 2000 (in Japanese).

[10] K. Yamane and Y. Nakamura, "Dynamics Filter - Concept and Implementation of On-Line Motion Generator for Human Figures," *IEEE Transactions on Robotics and Automation*, vol.19, No.3, pp.421-432, 2003.

[11] M. Kouchi, M. Mochimaru, H. Iwasawa and S. Mitani, "Anthropometric database for Japanese Population 1997-98," Japanese Industrial Standards Center (AIST, MITI), 2000.

[12] Y. Fujimoto and A. Kawamura, "Three Dimensional Digital Simulation and Autonomous Walking Control for Eight-Axis Biped Robot," *Proceedings of IEEE International Conference on Robotics and Automation*, pp.2877-2884, 1995.

[13] J.Y.S. Luh, M.W. Walker and R.P.C. Paul, "On-Line Computational Scheme for Mechanical Manipulators," *ASME Journal of Dynamics Systems, Measurement, and Control*, Vol.102, No.2, pp.69-76, 1980.

[14] M.W. Walker and D.E. Orin, "Efficient Dynamic Computer Simulation of Robotic Mechanisms," *ASME Journal of Dynamics Systems, Measurement, and Control*, Vol.104, pp.205-211, 1982.

[15] T. Mita and K. Osuka, "Introduction to Robot Control," CORONA PUBLISHING CO., LTD., 1989 (in Japanese).

[16] N. Hogan, "Impedance Control; An Approach to Manipulation, Parts I-III," *ASME Journal of Dynamics Systems, Measurement, and Control* Vol.107, No.1, pp.1-24, 1985.

[17] W. Song, M. Minami, F. Yu, Y. Zhang and A. Yanou, "3-D Hand & Eye-Vergence Approaching Visual Servoing with Lyapunov-Stable Pose Tracking," *Proceedings of IEEE International Conference on Robotics and Automation*, pp.5210-5217, 2011.

[18] F. Yu, W. Song and M. Minami, "Visual Servoing with Quick Eye-Vergence to Enhance Trackability and Stability," *Proceedings of IEEE/RSJ International Conference on Intelligent Robots and Systems*, pp.6228-6233, 2010.

[19] T. Maeba, M. Minami, A. Yanou and J. Nishiguchi, "Dynamical Analyses of Humanoid's Walking by Visual Lifting Stabilization Based on Event-driven State Transition", 2012 IEEE/ASME Int. Conf. on Advanced Intelligent Mechatronics Proc., pp.7-14, 2012.